

Coherent Control of Resonant Two-Photon Transitions by Counter-Propagating Ultrashort Pulse Pairs

Woojun Lee, Hyosub Kim, Kyungtae Kim, and Jaewook Ahn

Department of Physics, KAIST, Daejeon 305-701, Korea

(Dated: October 11, 2024)

We describe optimized coherent control methods for two-photon transitions in atoms of a ladder-type three-state energy configuration. Our approach is based on the spatial coherent control scheme which utilizes counter-propagating ultrashort laser pulses to produce complex excitation patterns in an extended space. Since coherent control requires constructive interference of constituent transition pathways, applying it to an atomic transition with a specific energy configuration requires specially designed laser pulses. Here, we show, in an experimental demonstration, that the two-photon transition with an intermediate resonant energy state can be coherently controlled and retrieved out from the resonance-induced background, when phase-flipping of the laser spectrum near the resonant intermediate transition is used. A simple reason for this behavior is the fact that the transition amplitude function (to be added to give an overall two-photon transition) changes its sign at the intermediate resonant frequency, thus, by a proper spectral-phase programming, the excitation patterns (or the position-dependent interference of the transition given as a consequence of the spatial coherent control) are well isolated in space along the focal region of the counter-propagating pulses.

PACS numbers: 32.80.Qk, 78.47.jh, 42.65.Re

I. INTRODUCTION

Femtosecond laser optics has been widely used, during the last two decades, as a time-resolving spectroscopic means in studying ultrafast time-scale dynamics of variety of quantum systems including atoms, molecules, quasi-particles in solids, etc [1–5]. Extreme peak intensity of femtosecond laser pulses has also enabled high-order nonlinear optical processes such as multi-photon excitations, high-harmonic generations, and above-threshold ionizations, to list a few [6–9]. Besides these usages, coherent control [10–12], the technique of using laser pulse shapes to steer quantum processes towards certain desirable outcomes, has gradually become another important use of femtosecond laser and the information of such laser pulse shapes as obtained through coherent control often plays a crucial role in understanding the quantum structure of the materials under consideration [13–16]. In that regards, people can furthermore analytically design the laser pulse shapes optimized, although limited to a few quantum systems, for more selective and efficient nonlinear optical processes [17–22].

The recent demonstration [23] that a counter-propagating pair of ultrafast laser pulses coherently induces Doppler-free two-photon transitions of atoms shows an intriguing possibility towards ultra-precision spectroscopy [24], especially when being used in conjunction with the femtosecond frequency comb [25, 26]. This method, termed as spatial coherent control, coherently arranges in time the spectral components of the laser pulse in such a way that all the counter-propagating photon pairs, energy-resonant to the atomic transition (*i.e.*, $\hbar\omega_1 + \hbar\omega_2 = E_e - E_g$), collide only at specific locations along the beam direction. Since the resonance condition varies from one atom species to the another, the atom-

specific spectroscopic information can be retrieved by imaging the distinct, if a proper coherent control scheme is used, spatial excitation profile. So far, this powerful method of spatial coherent control has been applied being limited to non-resonant two-photon transitions (or to the cases in which intermediate states are not directly involved with the transition) and yet to resonant two-photon transitions (two-photon transitions with a resonant intermediate state or states). However, there already exist sophisticated pulse-shaping methods [17, 22] to deal with the latter case, the resonant two-photon transitions, in the context of optimized single-pulse controls toward enhanced two-photon transitions.

In this paper, we describe an experimental demonstration of the spatial coherent control of the resonant two-photon transition $5S_{1/2} \rightarrow 5P_{2/3} \rightarrow 5D$ of atomic rubidium (^{85}Rb). Ultrashort laser pulses are programmed in such a way that not only (1) counter-propagating photon pairs, and no photon pairs in the same propagation direction, induce the given transition, but also (2) the contributions from the all possible combinations of photon energies, involving such transition, are coherently added for an optimal net transition probability. For this, we first adopt spectral pulse shaping methods: V-shape spectral phase programming for the condition (1); and either a spectral phase-step or a spectral phase-window for (2) in the first and second experiments, respectively. In the last experiment, we use a spectral phase shaping method to further enhance the net two-photon transition, in which the spectral amplitude for the resonant intermediate transition is blocked so that the the spatially extended excitation caused by sequential two-photon transitions through the intermediate resonant state is avoided.

In the remaining sections, we first theoretically sketch

the laser pulse shaping ideas relevant for the resonant and non-resonant two-photon transitions, respectively, in Sec. II, before the experimental procedure is described in Sec. III. We then present the experimental result of the spatial coherent control of the two-photon transition of ^{85}Rb in Sec. IV and conclude in Sec. V.

II. THEORETICAL CONSIDERATION

We consider a pair of laser pulses, denoted by $\mathcal{E}_1(z, t)$ and $\mathcal{E}_2(z, t)$, respectively propagating along $\pm z$ directions, interacts with a three-level atom in a ladder-type energy configuration. The two-photon transition amplitude from the ground state $|g\rangle$ to the final state $|e\rangle$ through the intermediate state $|i\rangle$ is then obtained from the second-order Dyson series in the perturbative interaction regime as

$$c_{eg}(z, t) = -\frac{\mu_{ei}\mu_{ig}}{2\pi\hbar^2} \int_{-\infty}^t dt_1 e^{i\omega_{ei}t_1} \mathcal{E}(z, t_1) \times \int_{-\infty}^{t_1} dt_2 e^{i\omega_{ig}t_2} \mathcal{E}(z, t_2), \quad (1)$$

where $\mathcal{E}(z, t) = \mathcal{E}_1(z, t) + \mathcal{E}_2(z, t)$ and μ_{ei} and μ_{ig} are the corresponding dipole moments. The integration provides the transition amplitude in terms of the spectral amplitudes (including phase) $E_1(\omega) = FFT[\mathcal{E}_1(0, t)]$ and $E_2(\omega) = FFT[\mathcal{E}_2(0, t)]$ by

$$c_{eg}(z) = i\frac{\mu_{ei}\mu_{ig}}{\hbar^2} \left[i\pi E(\omega_{ig})E(\omega_{ei}) + \int_{-\infty}^{\infty} \frac{E(\omega)E(\omega_{eg}-\omega)}{\omega_{ig}-\omega} d\omega \right], \quad (2)$$

where $E(\omega) = E_1(\omega)e^{-i\omega z/c} + E_2(\omega)e^{i\omega z/c}$ and $t \rightarrow \infty$ is assumed. We denote the first term in the bracket of Eq. (2) by $c_r(z)$, the resonant two-photon transition, and the second term by $c_{nr}(z)$, the non-resonant two-photon transition, *i.e.*,

$$c_{eg}(z) = c_r(z) + c_{nr}(z). \quad (3)$$

which can be respectively written down in terms of $E_1(\omega)$ and $E_2(\omega)$ as

$$c_r(z) = -\pi\frac{\mu_{ei}\mu_{ig}}{\hbar^2} [E_1(\omega_{ig})E_1(\omega_{ei}) + E_2(\omega_{ig})E_2(\omega_{ei})e^{2i\omega_{eg}z/c} + E_1(\omega_{ig})E_2(\omega_{ei})e^{2i\omega_{ei}z/c} + E_2(\omega_{ig})E_1(\omega_{ei})e^{2i\omega_{ig}z/c}], \quad (4)$$

$$c_{nr}(z) = i\frac{\mu_{ei}\mu_{ig}}{\hbar^2} \int_{-\infty}^{\infty} \frac{d\omega}{\omega_{ig}-\omega} [E_1(\omega)E_1(\omega_{eg}-\omega) + E_2(\omega)E_2(\omega_{eg}-\omega)e^{2i\omega_{eg}z/c} + E_1(\omega)E_2(\omega_{eg}-\omega)e^{2i(\omega_{eg}-\omega)z/c} + E_2(\omega)E_1(\omega_{eg}-\omega)e^{2i\omega z/c}]. \quad (5)$$

Note that the first two terms in each bracket in Eqs. (4) and (5) are the single-pulse contributions from either direction of the pulse propagations, and the last two terms are caused by the presence of both pulses. Furthermore, the all terms in $c_r(z)$ and the first two terms (the single-pulse contribution) in $c_{nr}(z)$ have the position-dependent phase factors ($1, e^{2i\omega_{eg}z/c}, e^{2i\omega_{ei}z/c}, e^{2i\omega_{ig}z/c}$, etc.) that are not directly coupled with the laser spectrum ω , while

the last two terms (the non-resonant transition contribution by the presence of the both pulses) in $c_{nr}(z)$ has explicit correlation between the position coordinate z and the laser spectrum ω , which means that the last two terms in $c_{nr}(z)$, and no other terms, contribute to the excitation profile.

The position dependent part of the excitation spatial profile is approximately given by

$$S(z) \propto \left| \int_{-\infty}^{\infty} \frac{d\omega A(\omega)A(\omega_{eg}-\omega)}{(\omega_{ig}-\omega)(\omega_{ei}-\omega)} e^{i[\Phi(\omega)+\Phi(\omega_{eg}-\omega)+2i\omega z/c]} d\omega \right|^2, \quad (6)$$

where the spectral amplitude function $A(\omega)$ and the spectral phase function $\Phi(\omega)$ are defined the same for the both pulses, when they are split from a single laser pulse, as

$$E_1(\omega) = E_2(\omega) = A(\omega)e^{i\Phi(\omega)}. \quad (7)$$

Therefore, in the context of the spatial coherent control, the phase function $\Phi(\omega)$ can be programmed in such a way that the two-photon transition components in the integral calculation in Eq. (6) satisfy a constructive in-

interference condition only at specific positions, so that the excitation spatial profile $S(z)$ can be used as a spectroscopic means.

III. EXPERIMENTAL DESCRIPTION

The experimental setup is schematically shown in Fig. 1(a). Femtosecond optical pulses were generated from a conventional Ti:sapphire laser oscillator (of a cavity length $L = 1.75$ m) mode-locked around the center frequency set to the two-photon transition frequency (*i.e.* $\omega_o = \omega_{eg}/2$). The laser bandwidth (FWHM) was 25 nm in wavelength scale. The pulses were then spectrally resolved in a $4f$ -geometry Fourier plane and phase-modulated by a 128-pixel spatial-light modulator (SLM) [27] to program $\Phi(\omega)$. The focal length of the $4f$ -geometry was 200 mm and the groove number of both gratings was 1200 mm^{-1} [28]. The width of each pixel in SLM was $100 \mu\text{m}$ and the pulse bandwidth incident into each pixel was 0.37 nm in wavelength scale. After pulse-shaping, the pulses were focused in a rubidium vapor cell (^{85}Rb) located at $z = 0$, de-focused, collimated, and then reflected back by a mirror located at $z = L$, so that each counter-propagating laser pulse collided with the next pulse in the vapor cell. The focal length of both focusing lenses was 200 mm. The beam diameter and the Rayleigh range of the focus were $100 \mu\text{m}$ and 10 mm, respectively.

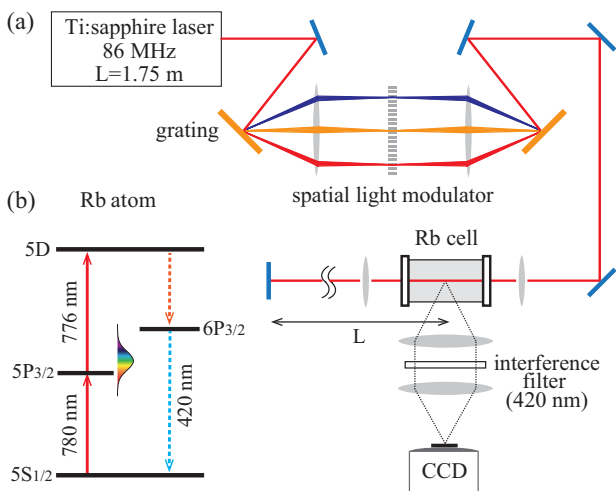


FIG. 1: (Color online) (a) Schematic diagram of the experimental setup. Ultrafast laser pulses were programmed by a spatial light modulator to interact with rubidium atoms in a colliding pulse geometry. The cavity length $L = 1.75$ m of the laser was matched with the extra travel of the reflected pulses. (b) The energy level diagram of atomic rubidium excited from $5S_{1/2}$ to $5D$ and the fluorescence from $6P_{3/2}$ was monitored.

The ^{85}Rb atoms were two-photon excited from the ground state $|g\rangle=5S_{1/2}$ to the final state $|e\rangle=5D$ via the intermediate state $|i\rangle=5P_{3/2}$ [see Fig. 1(b)]. The

corresponding frequencies (wavelengths) were $\omega_{ig}/2\pi = 384.6 \text{ THz}$ ($\lambda_{ig} = 780 \text{ nm}$), $\omega_{ei}/2\pi = 386.6 \text{ THz}$ ($\lambda_{ei} = 776 \text{ nm}$), and $\omega_o/2\pi = 385.6 \text{ THz}$ ($\lambda_o = 778 \text{ nm}$), respectively [29]. Note that the $D1$ transition to $5P_{1/2}$ state was out of the laser spectral range. The excited atoms in the $5D$ were decayed to $6P$, and the spatial profile of the fluorescence at 420 nm ($5P \rightarrow 5S_{1/2}$) were imaged by a CCD camera through one-to-one telescope imaging by a pair of $f = 25 \text{ mm}$ lenses. The image resolution of the camera was $4.54 \mu\text{m}$.

IV. RESULTS AND DISCUSSION

Before the result of the resonant-two-photon experiments is presented, we first consider the *non-resonant two-photon transition* case, which is the case when the intermediate state $|i\rangle$ is out of the laser spectral range (*i.e.*, $\omega_{ig} < \omega_{\min}$ for $\omega_{ig} < \omega_{ei}$). The V -shape spectral phase function defined in Ref. [23] as

$$\Phi_V(\omega) = \alpha|\omega - \omega_o|, \quad (8)$$

makes two distinct local functions in the spatial excitation profile $S(z)$ in Eq. (6), which are conceptually given by

$$S(z) \propto \delta(z - z_o) + \delta(z + z_o), \quad (9)$$

where $z_o = \alpha c$ is a constant determined by the phase slope $\alpha = |d\Phi_V/d\omega|$ and $\delta(z)$ is a Dirac delta function. However, when this phase function $\Phi_V(\omega)$ is used for the resonant two-photon case, the image appears as in Fig. 2(a) if $\alpha < 0$. The darker region in $z < |z_o|$ violates the causality for the resonant two-photon transition, or the $|g\rangle \rightarrow |i\rangle$ occurs later in time than $|i\rangle \rightarrow |e\rangle$. When $\alpha > 0$, spatial excitation pattern is not formed at all.

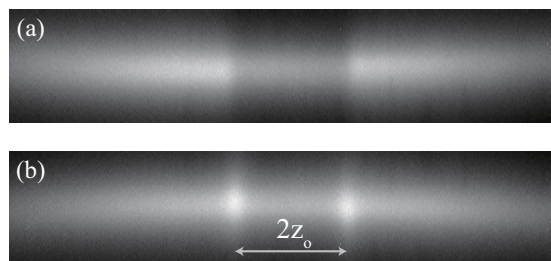


FIG. 2: (Color online) Photo images of the fluorescence signals: (a) A V -shape spectral phase function $\Phi_V(\omega)$ is used with $\alpha = -1.4 \text{ ps}$, (b) The spectral phase function with the V -shape and a phase step $\Phi_1(\omega)$ is used with $\beta = \pi$. [$\Phi_V(\omega)$ and $\Phi_1(\omega)$ are defined in Eqs. (8) and (10), respectively, and $z_o = 420 \mu\text{m}$.]

On the other hand, in the *resonant two-photon transition* case, or the case when the intermediate state is located within the laser spectrum (*i.e.*, $\omega_{\min} < \omega_{ig} < \omega_{\max}$ directly involved with the two-photon transition, alternative phase functions can be used to deal with the resonant

transitions to $|i\rangle$. For example, the image in Fig. 2(b) was taken with the following phase function:

$$\Phi_1(\omega) = \alpha|\omega - \omega_o| + \beta\Theta(\omega - \omega_{ig}), \quad (10)$$

with the Heaviside step function defined by $\Theta(x) = 1$ for $x \geq 0$ and 0 for $x < 0$. The physics behind this behavior is from the dispersion term $1/(\omega_{ig} - \omega)$ in Eq. (6), which causes a phase flip across the resonant intermediate-state frequency and results in a destructive interference among the two-photon transition pathways in the given spectral sum. However, the second phase-step term $\beta\Theta(\omega - \omega_{ig})$ in Eq. (10) recovers the constructive interference. The π -step phase function, or a similar concept, has been tested before in simple coherent control experiments of two-photon transitions with one or two resonant intermediate states [17, 22].

Figure 3 compares the experimental result of the first experiment [$\Phi_1(\omega)$] with a corresponding numerical calculation. By maintaining the phase slope value fixed at $\alpha = -1.4$ ps, the phase step value was changed from $\beta = 0$ to 2π , and the fluorescence signals (measured along z direction where the position is shown in the horizontal axis) were plotted as a function of β (along the vertical axis) in Fig. 3(a). As expected, sharp fluorescence peaks appear at $z = z_o$ and $-z_o$, when $\beta = \pi$ is applied. The spatial excitation profiles measured at $\beta = 0$ (blue dash-dot line) and π (red line) are respectively shown in Fig. 3(c). This experimental result agrees well with the numerical simulation as shown in Figs. 3(b) and 3(d).

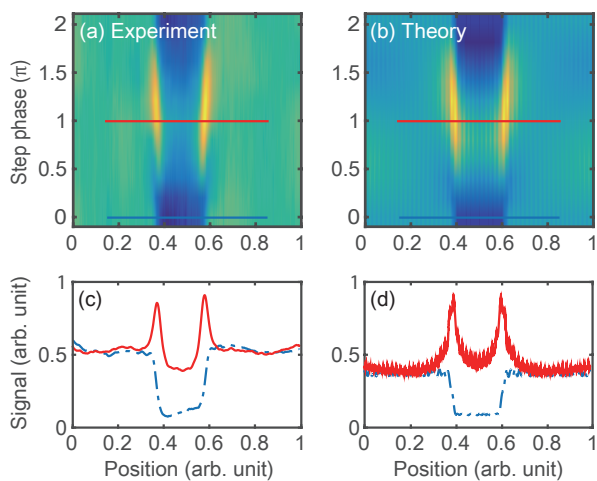


FIG. 3: (Color online) The first phase shaping experiment: (a, c) spatial fluorescence signals for $\Phi_1(\omega)$ (V -shape + phase step) spectral functions, (b,d) numerical simulation. Signals at $\beta = 0$ (blue dash-dot line) and π (red line) are extracted from (a) and (b) to show in (c) and (d), respectively. [Unwanted background signals due to the position-insensitive resonant two-photon transitions are subtracted for clarity by means of numerical fitting.]

In the second experiment, the spectral block between ω_{ig} and $\omega_{eg} - \omega_{ig}$ was phase-rotated from $\gamma = 0$ to π ,

i.e., the spectral phase function is given by

$$\Phi_2(\omega) = \alpha|\omega - \omega_o| + \gamma[\Theta(\omega - \omega_{ig}) - \Theta(\omega - \omega_{eg} + \omega_{ig})], \quad (11)$$

where the same $\alpha = -1.4$ ps was used as in the first experiment. This type of phase modulation is theoretically equivalent to the one in the first experiment, when $\gamma = \pi + \beta/2$ [22]. Both the $\Phi_1(\omega)$ in the first experiment and $\Phi_2(\omega)$ with $\gamma = \pi + \beta/2$ flip the sign of the dispersion term $1/(\omega_{ig} - \omega)(\omega_{ei} - \omega)$ in Eq. (6) in the spectral region $\omega_{ig} < \omega < \omega_{ei}$ with respect to the rest of the spectral region so that transitions from the whole spectral region become in phase. The result shown in Fig. 4 clearly shows the unresolved spatial profile at $\gamma = 0$ gradually becomes resolved as $\gamma \rightarrow \pi/2$. The maximal visibility is achieved at $\gamma = \pi/2$ in a good agreement with the theoretical prediction in Figs. 4(c) and 4(d).

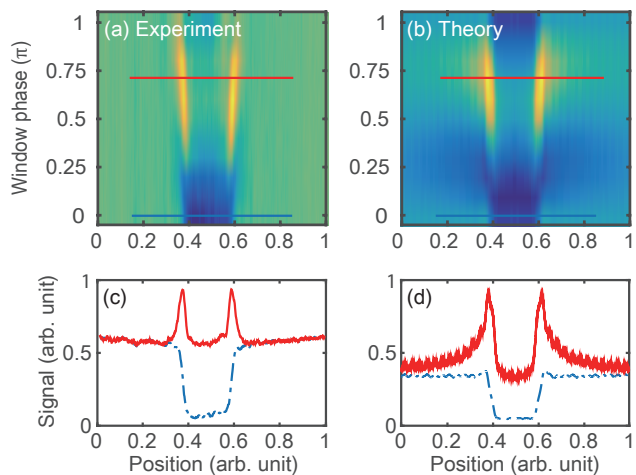


FIG. 4: (Color online) The second phase shaping experiment: (a, c) spatial fluorescence signals for $\Phi_2(\omega)$ (V -shape + phase block) spectral functions, (b,d) numerical simulation. Signals at $\gamma = 0$ (blue dash-dot line) and $\pi/2$ (red line) are extracted from (a) and (b) to show in (c) and (d), respectively.

Lastly, we used spectral amplitude shaping in addition to the spectral phase shaping in the first experiment, where the spectral components near the intermediate resonant transition ω_{ig} is removed. In this circumstance, the resonant transition from $5S_{1/2}$ state to $5P_{3/2}$ state is suppressed, so excitation only occurs at the points where the two photons respectively with frequencies ω_{ig} and $\omega_{eg} - \omega_{ig}$ collide with each other. The spectral phase modulation scheme in the first experiment, which is expressed as Eq. (10), was again applied, with the coefficient of the V -shape replaced by $\alpha = -0.8$ ps. Note that, as seen in Fig. 5(a), the excitation signals are localized at the points where the sub-pulses, separated by the V -shape phase, overlap at $z = \pm z_o$ with each other. Figs. 5(a) and 5(c) shows that the phase modulation with $\beta = \pi$ (red line) enhances and further localizes the peak signals over when only the bare V -shape is applied (blue

dash-dot line). This result again agrees well with the theoretical prediction in Figs. 5(b) and 5(d).

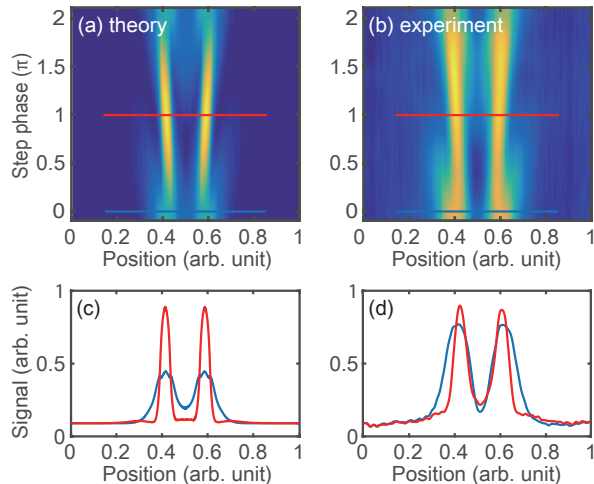


FIG. 5: (Color online) Amplitude + phase shaping experiment: (a,c) spatial fluorescence signals for $\Phi_1(\omega)$ (V-shape + phase step) spectral functions, with the intermediate resonant transition removed, (b,d) numerical simulation. Signals at $\beta = 0$ (blue dash-dot line) and $\pi/2$ (red line) are extracted from (a) and (b) to show in (c) and (d), respectively.

V. CONCLUSION

In conclusion, we have performed coherent control experiments of two-photon excitation of the ladder-type three-state atomic system, using counter-propagating phase-modulated ultrashort pulses. The laser pulses designed based on the spatial coherent control scheme to phase-flip the laser spectrum near the resonant intermediate transition have successfully produced spatially localized excitation patterns out from the resonance-induced background along the focal region of the counter-propagating pulses. The resulting constructive interference phenomena among the constitute non-resonant two-photon transitions are theoretically confirmed and verified by numerical calculations.

-
- [1] A. H. Zewail, *Angew. Chem. Int. Ed. Engl.* **39**, 2587 (2000).
- [2] P. Antoine, A. L’Huillier, and M. Lewenstein, *Phys. Rev. Lett.* **77**, 1234 (1996).
- [3] J. Ahn, D. N. Hutchinson, C. Rangan, and P. H. Bucksbaum, *Phys. Rev. Lett.* **86**, 1179 (2001).
- [4] G. C. Cho, W. Kutt, and H. Kurz, *Phys. Rev. Lett.* **65**, 764 (1990).
- [5] T. K. Cheng, S. Vidal, M. J. Zeiger, G. Dresselhaus, M. S. Dresselhaus, and E. P. Ippen, *Appl. Phys. Lett.* **59**, 1923 (1991).
- [6] T. Brabec and F. Krausz, *Rev. Mod. Phys.* **72**, 545 (2000).
- [7] R. R. Freeman, P. H. Bucksbaum, H. Milchberg, S. Darack, D. Schumacher, and M. E. Geusic, *Phys. Rev. Lett.* **59**, 1092 (1987).
- [8] P. B. Corkum, *Phys. Rev. Lett.* **71**, 1994 (1993).
- [9] P. Agostini and L. F. DiMauro, *Rep. Prog. Phys.* **67**, 813 (2004).
- [10] K. Bergmann, H. Theuer, and B. W. Shore, *Rev. Mod. Phys.* **70**, 1003 (1998).
- [11] M. Shapiro and P. Brumer, *Principles of the quantum control of molecular processes*, (Wiley, New York, 2003).
- [12] D.J. Tanner and S. A. Rice, *J. Chem. Phys.* **83**, 5013 (1985).
- [13] R. Bartels, S. Backus, E. Zeek, L. Misoguti, G. Vdovin, I. P. Christov, M. M. Murnane, and H. C. Kapteyn, *Nature* **406**, 164 (2000).
- [14] J. L. Herek, W. Wohlleben, R. J. Cogdell, D. Zeidler, and M. Motzkus, *Nature* **417**, 533535 (2002).
- [15] J. M. Dela Cruz, I. Pastirk, M. Comstock, V. V. Lozovoy, and M. Dantus, *Proc. Natl. Acad. Sci.* **101**, 16996 (2004).
- [16] V. I. Prokhorenko, A. M. Nagy, S. A. Waschuk, L. S. Brown, R. R. Birge, and R. J. Dwayne Miller, *Science* **313**, 1257 (2006).
- [17] N. Dudovich, B. Dayan, S. M. GallagherFaeder, and Y. Silberberg, *Phys. Rev. Lett.* **86**, 47 (2001).
- [18] S. D. Clow, C. Trallero-Herrero, T. Bergeman, and T. Weinacht, *Phys. Rev. Lett.* **100**, 233603 (2008).
- [19] M. Reetz-Lamour, T. Amthor, J. Deiglmayr, and M. Weidemüller, *Phys. Rev. Lett.* **100**, 253001 (2008).
- [20] S. Lee, J. Lim, C. Y. Park, and J. Ahn, *Opt. Express* **19**, 2266 (2011).
- [21] J. Lim, H. G. Lee, J. U. Kim, S. Lee, and J. Ahn, *Phys. Rev. A* **83**, 053429 (2011).
- [22] H. G. Lee, H. Kim, J. Lim, and J. Ahn, *Phys. Rev. A* **88**, 053427 (2013).
- [23] I. Barmes, S. Witte, and K. S. E. Eikema, *Nat. Photonics* **7**, 38 (2013).
- [24] I. Barmes, S. Witte, and K. S. E. Eikema, *Phys. Rev. Lett.* **111**, 023007 (2013).
- [25] R. Holzwarth, Th. Udem, T. W. H’ansch, J. C. Knight, W. J. Wadsworth, and P. St. J. Russell, *Phys. Rev. Lett.* **85**, 2264 (2000).
- [26] D. J. Jones, S. A. Diddams, J. K. Ranka, A. Stentz, R. S. Windeler, J. L. Hall, and S. T. Cundiff, *Science* **288**, 635 (2000).
- [27] A. M. Weiner, *Rev. Sci. Inst.* **71**, 1929 (2000).
- [28] R. L. Fork, O. E. Martinez, and J. P. Gordon, *Opt. Lett.* **9**, 150 (1984).

- [29] J. E. Sansonetti, *J. Phys. Chem. Ref. Data*, **35**, 301 (2006).